

5-17-2022

## Microseismic source locating method based on variable step size accelerated search

Bao-xin JIA

*Liaoning Key Laboratory of Mine Subsidence Disaster Prevention and Control, Liaoning Technical University, Fuxin, Liaoning 123000, China*

Feng LI

*School of Civil Engineering, Liaoning Technical University, Fuxin, Liaoning 123000, China*

Yi-shan PAN

*School of Environment, Liaoning University, Shenyang, Liaoning 110036, China*

Lin-li ZHOU

*School of Civil Engineering, Liaoning Technical University, Fuxin, Liaoning 123000, China*

Follow this and additional works at: <https://rocksoilmech.researchcommons.org/journal>



Part of the [Geotechnical Engineering Commons](#)

---

### Custom Citation

JIA Bao-xin, LI Feng, PAN Yi-shan, ZHOU Lin-li, . Microseismic source locating method based on variable step size accelerated search[J]. Rock and Soil Mechanics, 2022, 43(3): 843-856.

This Article is brought to you for free and open access by Rock and Soil Mechanics. It has been accepted for inclusion in Rock and Soil Mechanics by an authorized editor of Rock and Soil Mechanics.

## Microseismic source locating method based on variable step size accelerated search

JIA Bao-xin<sup>1,2</sup>, LI Feng<sup>1</sup>, PAN Yi-shan<sup>3</sup>, ZHOU Lin-li<sup>1</sup>

1. School of Civil Engineering, Liaoning Technical University, Fuxin, Liaoning 123000, China

2. Liaoning Key Laboratory of Mine Subsidence Disaster Prevention and Control, Liaoning Technical University, Fuxin, Liaoning 123000, China

3. School of Environment, Liaoning University, Shenyang, Liaoning 110036, China

**Abstract:** Microseismic locating method is an important part of microseismic monitoring technology, the key of which is to locate the hypocenter. In this study, we analyze the two- and three-dimensional spatial distributions of microseismic locating objective functions through spatial gridding and calculation of the objective function values of grid intersections. Accordingly, we find that the objective function is continuous with a unique minimum value, the convergence range of single axis decreases gradually, and the convergence range of each axis varies. Using the above findings and the advantages and disadvantages of pattern search method and grid search method, we propose a variable step size accelerated search method based on continuous comparison module, the variable step size module and the acceleration module. Through the comparison of four indices between the simulation example and the engineering data, i.e. the convergence stability, the accuracy of the results, the calculation speed, and the degree of influence for initial values of parameters, we can find that in the simulation example, compared with simulated annealing algorithm and genetic algorithm, the standard deviations of objective function value, locating error and wave velocity error of the variable step size accelerated search method are all 0. The average locating error of the proposed search method is 0.7% and 1.9% of that of other two algorithms, respectively. The average calculation time of the proposed search method is 6.9% and 33.2% of that of the other two algorithms, respectively. The influence of merely changing one parameter on the locating error in this method is between 0.005 m and 0.025 m. Reducing the lower limit of the search step size can effectively improve the accuracy of the results but increase calculation time. When the first arrival time, objective function model and coordinates of the geophone position are specified, the search algorithm has negligible impact on the locating accuracy.

**Keywords:** microseismic locating; spatial image; variable step size accelerated search method; simulated annealing algorithm; genetic algorithm

### 1 Introduction

With the rapid development of economy, China's demands for various mineral resources are increasing. Due to the uncertainty of the underground environment where the mining is located, the mining of mineral resources is accompanied by a series of environmental hazards, such as pressure bump, goaf collapse, rockburst and rib spalling and roof collapse of roadways<sup>[1–3]</sup>.

Microseismic monitoring technology is generally used to monitor and locate the sources of accidents in the mining of mineral resources. The microseismic source locating method is the core content of microseismic monitoring and the key to improving the prediction accuracy<sup>[4–5]</sup>. Improving the locating accuracy of microseismic source locating method is always a challenging issue for microseismic monitoring technology.

In the microseismic source locating method, the position and time of the microseismic event are obtained through the microseismic signals collected by the geophone<sup>[6]</sup>.

At present, scholars at home and abroad improve the source locating accuracy mainly by integrating or improving conventional microseismic locating methods. Li et al.<sup>[7]</sup> proposed a simplex locating method based on L1 norm statistics, which has a high anti-interference for outliers with large deviations. Jia et al.<sup>[8]</sup> used high-density arrays and particle swarm optimization to analyze the relationship between the locating error and the number and position of sensors. Wang et al.<sup>[9]</sup> proposed a differential evolution microseismic locating method which improves the objective function to solve the problem that conventional locating methods rely too much on the accuracy of travel time. Wang et al.<sup>[10]</sup> proposed a combined microseismic source locating method based on simplex-shortest path ray tracing. Jiang et al.<sup>[11]</sup> proposed a microseismic source locating algorithm based on grid search-Newton iteration method using gridding of monitoring area and Newton iteration method. Soledad et al.<sup>[12]</sup> proposed an improved global optimization algorithm by optimizing the azimuth, accompanied with annealing algorithm and particle swarm

Received: 10 June 2021

Revised: 30 December 2021

This work was supported by the National Natural Science Foundation of China(51774173), the Discipline Innovation Team of Liaoning Technical University (LNTU20TD08), the "Rejuvenating Liaoning Talents Plan" Project of Liaoning Province(XLYC2007163) and the Liaoning BaiQianWan Talents Program.

First: JIA Bao-xin, male, born in 1978, PhD, Professor, research interests: mine disaster mechanics. E-mail: [jbx\\_811010@126.com](mailto:jbx_811010@126.com)

optimization. Neale et al.<sup>[13]</sup> proposed an improved multi-array seismic source inversion locating method by optimizing the spatial layout of the station. Xiao et al.<sup>[14]</sup> proposed a cross-difference inversion method for micro-seismic locating with real-time update velocity model, using the initial arrival time of P- and S-waves. Nan et al.<sup>[15]</sup> proposed the principle of optimization of geophone network that can improve the locating accuracy by studying the spatial layout and placement orientation of geophone arrays.

The above research results have improved the source locating accuracy to a certain extent, but there are still some shortcomings. For example, the above methods rely on the selection of initial parameters for iteration. Improper selection may lead to distortion or divergence of calculation results of locating<sup>[16]</sup>. Due to the fixed search step size, the locating results may show low accuracy or poor convergence. For different objective functions and initial data (including coordinates of the geophone and the first arrival time of P-wave), poor stability of the locating result or calculation speed may occur.

Therefore, we use spatial gridding and calculation of objective function value of the grid intersection point. We analyze two- (2D) and three-dimensional (3D) spatial distributions of the objective function for microseismic event locating and obtain the convergence features of the objective function. Considering the above findings and the advantages and disadvantages of pattern search method and grid search method, we propose a variable step size accelerated search method based on the continuous comparison module, the variable step size module and the acceleration module. Finally, through the comparison of four indices between the simulation example and the engineering data, i.e. the convergence stability, the accuracy of the results, the calculation speed, and the degree of influence for the initial values of parameters, we demonstrate the effectiveness of the proposed search method.

## 2 Image analysis of microseismic locating objective function

The source locating method based on travel time residual theory is widely used to locate the microseismic events<sup>[17–18]</sup>. The difference between the calculated travel time and the actual observed time is the travel time residual, which can be used to derive the microseismic locating objective function according to certain rules. In this paper, the spatial image of the objective function is drawn by the method of spatial gridding, so as to explore the spatial distribution

features of the objective function and provide a theoretical basis for the design of the locating algorithm.

### 2.1 Design of objective function

Due to the obvious response of the first arrival of the P-wave seismic phase, it is easy to accurately determine the arrival time. Therefore, we introduce the calculation formula of the travel time residual for the P-wave seismic phase, which takes the mathematical expectation of the difference of the theoretically calculated travel time and the actual observed time as the estimated origin time<sup>[19]</sup>:

$$t_p^i = \sqrt{(x_i - x_0)^2 + (y_i - y_0)^2 + (z_i - z_0)^2} / v_0 \quad (1)$$

$$T_{p0} = \frac{1}{N} \sum_{i=1}^N (T_p^i - t_p^i) \quad (2)$$

$$R(x_0, y_0, z_0, v_0) = \sqrt{\frac{1}{N} \sum_{i=1}^N (T_p^i - t_p^i - T_{p0})^2} \quad (3)$$

where  $t_p^i$  is the theoretically calculated travel time (s);  $x_i$ ,  $y_i$  and  $z_i$  are the coordinates of each geophone (m);  $v_0$  is the average velocity of the P-wave from the source  $O(x_0, y_0, z_0)$  to each geophone (m/s);  $T_{p0}$  is the estimated origin time (s);  $T_p^i$  is the observed arrival time (s); and  $N$  is the number of geophones.

In this paper, Eq.(3) is taken as the objective function. There are four unknowns, which are the  $X$ -axis coordinate  $x_0$  of the source  $X$ , the  $Y$ -axis coordinate  $y_0$  of the source  $Y$ , the  $Z$ -axis coordinate  $z_0$  of the source  $Z$ , and the average P-wave velocity  $v_0$ . In order to improve the locating accuracy, instead of pre-setting the magnitude of the average P-wave velocity  $v_0$ , we use the unknown  $v_0$  and the unknown coordinates of the source for joint calculation<sup>[20]</sup>. Then we analyze its influence on the objective function. For complex velocity models, the average wave velocity calculated simultaneously with the coordinates of the source in the variable step size accelerated search method can also be in function form. For example, in simplified layered geological conditions, it can be a piecewise function; or in a known wave velocity field conditions, it can be a variable wave velocity that is straight-line propagation.

The closer the objective function value approaches 0, the more accurate the locating result is. When the objective function fails to converge or the value is large, it indicates that the source cannot be located or the error is large. The search algorithm is used to find its minimum value. The spatial position corresponding to the minimum value is the epicenter. Therefore, the microseismic source locating can be transformed into finding the variable values corresponding to the minimum value of the multivariate

objective function under the convergence condition.

**2.2 Spatial distribution of objective function with given data**

From Eq.(3), we can draw the spatial image of the objective function  $R(x_0, y_0, z_0, v_0)$  based on its continuity. After inputting the initial data such as the coordinates of each geophone and the first arrival time of P-wave, the spatial distribution of the function can be obtained by spatial gridding and calculation of the objective function value of the grid intersections.

We take the data from Zhang<sup>[21]</sup> as an example to illustrate the transformation of the objective function in space. The source  $M_4$  is selected. Its true coordinates are (800 m, 350 m, 600 m) and the true value of the average P-wave velocity is 5 m/ms. The coordinates of the geophone and the first arrival time of the P-wave are shown in Table 1.

**Table 1 Geophone coordinates and first arrival time of P-wave**

Serial number of geophone	Coordinates /m			First arrival time of P-wave /ms
	X	Y	Z	
A	0	0	0	246.896
B	0	0	1 000	227.093
C	1 000	0	1 000	148.578
D	1 000	0	0	179.568
E	1 000	1 500	0	297.488
F	0	1 500	0	339.795
G	0	1 500	1 000	326.376
H	1 000	1 500	1 000	281.779

Given that  $x_0, y_0$  and  $z_0$  are the spatial variables, and  $v_0$  is a velocity variable, the images are drawn with two combinations of both spatial variables, and spatial variables and velocity variables. In Figs.1–4,  $x_0$  ranges from 0 to 1 000 m,  $y_0$  ranges from 0 to 1 500 m,  $z_0$  ranges from 0 to 1 000 m, and  $v_0$  ranges from 3 m/ms to 20 m/ms.

**2.2.1 2D image of objective function**

(1) Image of  $R(x_0, y_0)$

From Fig.1, we find that the objective function  $R(x_0, y_0)$  is a continuous function with an obvious unique minimum value when  $v_0$  is 5 m/ms and  $z_0$  is 600 m. When the objective function value is in the range of 0 to 20, the convergence ranges of  $x_0$  and  $y_0$  are 590–1 080 m and 190–500 m, respectively.

(2) Image of  $R(x_0, v_0)$

From Fig.2, we find that when  $y_0$  is 350 m and  $z_0$  is 600 m, the image of the objective function  $R(x_0, v_0)$  is still continuous with an obvious unique minimum value. When the objective function value is in the range of 0 to 20,

the convergence ranges of  $x_0$  and  $v_0$  are 590–1 080 m and 3.7–7.5 m/ms, respectively.

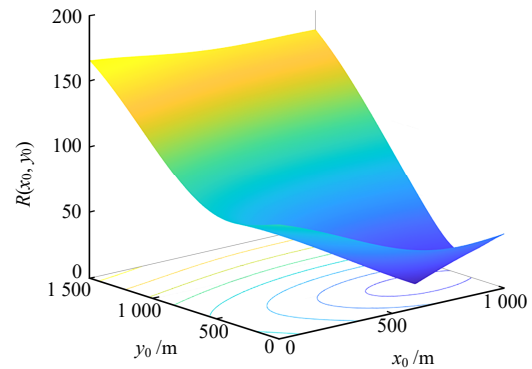


**Fig. 1 Image of  $R(x_0, y_0)$  when  $v_0$  and  $z_0$  are fixed values**

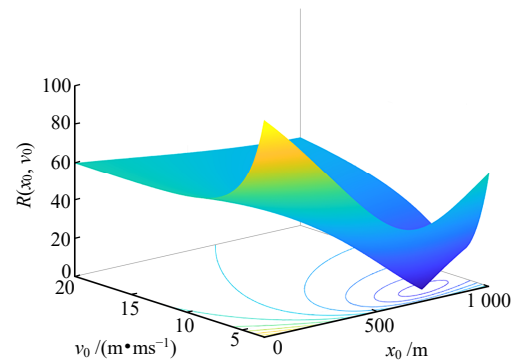


**Fig. 2 Image of  $R(x_0, v_0)$  when  $y_0$  and  $z_0$  are fixed values**

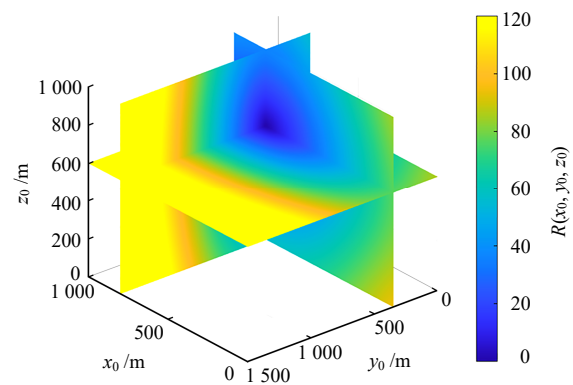


**Fig. 3 Image of  $R(x_0, y_0, z_0)$  when  $v_0$  is a fixed value**

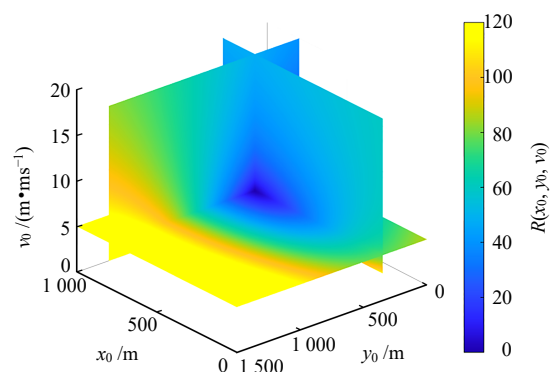


**Fig. 4 Image of  $R(x_0, y_0, v_0)$  when  $z_0$  is a fixed value**

### 2.2.2 3D image of objective function

The number of divisions  $F_s$  in Figs.3 and 4 is 100, and the observation angles are as follows: azimuth of  $-130^\circ$  and pitch angle of  $30^\circ$ .

#### (1) Image of $R(x_0, y_0, z_0)$

The 3D image is shown in this part in slice. The three-axis slices are at  $x_0 = 800$  m,  $y_0 = 350$  m and  $z_0 = 600$  m. The objective function values are represented by different colors and the range is set from 0 to 120. The objective function  $R(x_0, y_0, z_0)$  when  $v_0$  is 5 m/ms is shown in Fig.3. When the objective function value is in the range of 0 to 15, the convergence range of  $x_0$  is from 660 m to 950 m, the convergence range of  $y_0$  is from 240 m to 450 m, and the convergence range of  $z_0$  is from 470 m to 730 m.

#### (2) Image of $R(x_0, y_0, v_0)$

The three-axis slices are at  $x_0 = 800$  m,  $y_0 = 350$  m and  $v_0 = 5$  m/ms. The objective function values are represented by different colors and the range is set from 0 to 120. The image of objective function  $R(x_0, y_0, v_0)$  when  $z_0 = 600$  m is shown in Fig.4. When the objective function value is in the range of 0 to 15, the convergence range of  $x_0$  is from 660 m to 950 m, the convergence range of  $y_0$  is from 240 m to 450 m, and the convergence range of  $v_0$  is from 3.4 m/ms to 9.2 m/ms.

### 2.2.3 Analysis of results

We find that the objective function has been continuous and the minimum value is unique in both 2D and 3D images. There is a clear downward trend around the minimum value. According to the above findings, a more efficient way to obtain the minimum value of the objective function is as follows: first, specify the overall search direction of the algorithm; then specify the multidirectional search, in which the search direction and step size can be slightly changed, they can be performed at the same time. They are performed simultaneously until the algorithm satisfies the iteration termination condition.

The following conclusions can be drawn from the above image analysis:

(1) The objective function is continuous and the minimum value is unique within the monitoring range. Instead of performing a wide-area random search, the function starts from a random point until it reaches the minimum point.

(2) The uniaxial convergence range narrows gradually. Since the starting point, the closer the iteration factor is to the source, the smaller the required search step size should be. Therefore, the search step size should adapt

to the change of the convergence range and cannot be a constant value.

(3) The convergence range of each axis is different. For each unknown of the objective function, its convergence range is different. Therefore, the search algorithm should take different search step sizes for each axis and adapt to the convergence range of each unknown.

## 3 The proposed variable step size accelerated search method

In this study, we propose a variable step size accelerated search method by taking the advantages of the pattern search method (fast directional search) and grid search method (variable search step size), and by improving the inability to adapt to the change of search progress in the pattern search method, and improving the complicated high-precision calculation process in the grid search method. Also, the conclusions obtained in Section 2 are incorporated to locate the source. This method can ensure that the iteration factor changes continuously, the search step size adapts to the change of the convergence range of each axis, and the search step size changes according to the convergence range. Using this method, we can continuously obtain the objective function values of each specified point of the polyhedron with the iteration factor being the geometric center, until the position of the minimum value of the objective function is found by iteration search.

### 3.1 Principle

The variable step size accelerated search method can be divided into three modules, i.e. the continuous comparison module, the variable step size module and the acceleration module. The continuous comparison module is the main process. The variable step size module and the acceleration module can change the step size for the main process.

#### 3.1.1 Continuous comparison module

Based on the uniqueness of the minimum value of the objective function, this module takes a starting point and continuously calculates and compares the objective function value of each specified point around each other.

When there are three unknowns, the position of specified points of the 3D polyhedron is shown in Fig.5, in which  $r$  is the initial value of the search step size (m). The 3D iteration process is shown in Fig.6. When there are four or more unknowns, it can be deduced to a four-dimensional space or a multi-dimensional space according to mathematical induction.

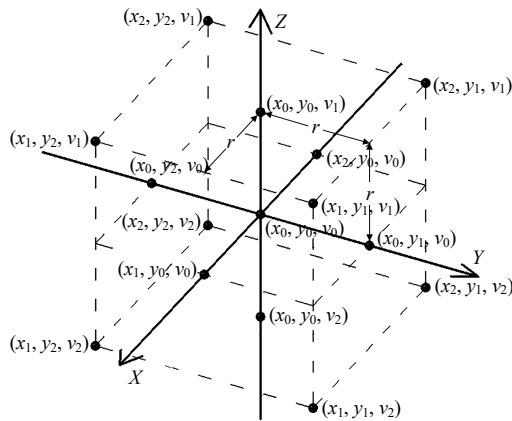


Fig. 5 Diagram of specified points of 3D polyhedron

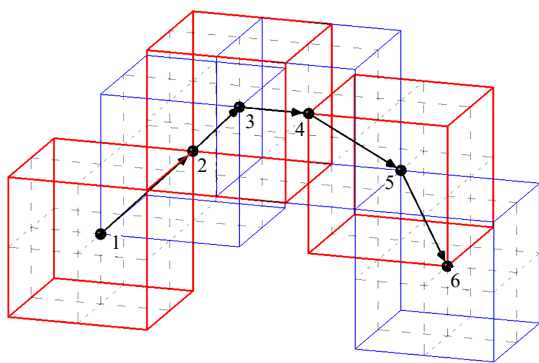


Fig. 6 Schematic diagram of 3D iterative process

### 3.1.2 Variable step size module

If the objective function value of a specified point is smaller than that of the starting point, its coordinates are assigned to the starting point. If no specified point is found to be smaller than that of the starting point in objective function values, the distance (search step size) from this point to each specified point is reduced to a half of the original value. The process continues until the search step size is smaller than the lower limit of the search step size. Finally, the final value is output.

### 3.1.3 Acceleration module

In actual calculation, the four variables are different in the value range and the convergence range. If a uniform search step size is set, there is a high probability that some variables have converged, while the rest continue to iterate gradually, which is a waste of calculation time. Therefore, the acceleration module is used to solve the above problem.

The principle of the acceleration module is to twice record the position number of the geometric center of the polyhedron reaching each specified point. If the two position numbers are the same, the search step size will be expanded to  $Q$  (acceleration coefficient) times the

original step size. Therefore, the convergence process of a single variable can be accelerated, thus speeding up the calculation. In the variable step size module, when the objective function values of specified points are all found to be higher than that of the starting point, the search step size will be reduced to a half of the original value. The above two modules have different control modes for the search step size. The termination condition of iteration of the algorithm is that the search step size is smaller than the lower limit. Therefore, in the acceleration module, the search step size should not be expanded excessively, avoiding offsetting the reduction of the search step size in the variable step size module. Thus the value of the acceleration coefficient of the search step size should be in the range of 1 to 2. The closer the value is to 2, the faster the calculation speed of the algorithm is, and vice versa. In practice, due to the irregular increase in the anisotropy of the spatial distribution of the objective function, a smaller acceleration coefficient can effectively improve the tolerated error when calculation errors arise as the search step size increases. Therefore, the acceleration coefficient in the range of 1.0–1.5 can better adapt to different convergence situations of the objective functions. In summary, the recommended acceleration coefficient is 1.5. The value can be adjusted according to the practical conditions.

## 3.2 Implementation

The procedure for the variable step size accelerated search method is described as follows:

(1) Read the position of each geophone and the P-wave arrival time, and execute Step (2).

(2) Input the following data: the initial coordinates of the starting point  $X_0(m)$ ,  $Y_0(m)$  and  $Z_0(m)$ ; the initial value of the average P-wave velocity  $V_0(m/s)$ ; the initial value of the search step size  $r$ ; the lower limit of the search step size  $J(m)$ ; the upper limit of model size  $X_u(m)$ ,  $Y_u(m)$  and  $Z_u(m)$ ; the lower limit of model size  $X_d(m)$ ,  $Y_d(m)$  and  $Z_d(m)$ ; the upper limit of speed  $V_u(m/s)$ ; the lower limit of speed  $V_d(m/s)$ ; the number of iterations  $I = 0$ ; the acceleration coefficient  $Q = 1.5$ ; the position information matrix  $F_c$  with all 0 elements in 1 row and 24 columns; the result record matrix  $P$  with all 0 elements in 1 row and 6 columns; and the position record matrix  $W_{ac}$  (empty matrix). Perform Step (3).

(3) Assign the initial coordinates  $X_0$ ,  $Y_0$ ,  $Z_0$  and  $V_0$  of the starting point to the coordinates  $x_0$ ,  $y_0$ ,  $z_0$  and  $v_0$  of the geometric center of the polyhedron, and execute

Step (4).

(4) Determine the relationship between the search step size  $r$  and the lower limit of the search step size  $J$ . If  $r > J$ , execute Step (5). If  $r < J$ , execute Step (19).

(5) Update the coordinates of each specified point of the polyhedron, and execute Step (6). The relationship between them and the geometric center of the polyhedron (the starting point in the first iteration) satisfies the following formula:

$$x_1 = x_0 + r \quad (4)$$

$$y_1 = y_0 + r \quad (5)$$

$$z_1 = z_0 + r \quad (6)$$

$$v_1 = v_0 + r \quad (7)$$

$$x_2 = x_0 - r \quad (8)$$

$$y_2 = y_0 - r \quad (9)$$

$$z_2 = z_0 - r \quad (10)$$

$$v_2 = v_0 - r \quad (11)$$

where  $x_1$  and  $x_2$  are the  $X$ -axis coordinates (m) of each specified point of the polyhedron;  $y_1$  and  $y_2$  are the  $Y$ -axis coordinates (m) of each specified point of the polyhedron;  $z_1$  and  $z_2$  are the  $Z$ -axis coordinates (m) of each specified point of the polyhedron; and  $v_1$  and  $v_2$  are the  $V$ -axis coordinates (m/s) of each specified point of the polyhedron.

(6) Calculate the objective function value  $R_0$  of the geometric center of the polyhedron, calculate  $R_1$  to  $R_{16}$  of specified points of the polyhedron, and calculate  $R_{17}$  to  $R_{24}$  of the intersections of the polyhedron and the coordinate axis. Execute Step (7).

(7) Determine in turn whether the independent variables  $x_j, y_k, z_l, v_m$  ( $j = 0, 1, 2; k = 0, 1, 2; l = 0, 1, 2; m = 0, 1, 2$ ) of  $R_i$  ( $i = 1, 2, \dots, 24$ ) in Step (6) satisfy  $X_d < X_j < X_u, Y_d < y_k < Y_u, Z_d < z_l < Z_u, V_d < v_m < V_u$  at the same time. If true, assign them to the  $i$ -th element of the position information matrix  $F_c$ . If not, set them to the maximum value of the floating point number. Execute Step (8).

(8) Sort the 24 elements of the position information matrix  $F_c$  in descending order. Find the last element number  $W_z$ . Record its value as the current minimum value  $R_{\min}$ . Execute Step (9).

(9) Determine the relationship between the current minimum value  $R_{\min}$  and the objective function value  $R_0$  of the geometric center of the polyhedron. If  $R_{\min} < R_0$ , execute Step (10). If  $R_0 > R_{\min}$ , execute Step (11).

(10) Assign  $I + 1$  to the number of iterations  $I$ . Assign

the element serial number  $W_z$  to the serial number  $i$ . Assign the coordinates of  $R_i$  to coordinates of the polyhedron geometric center  $x_0, y_0, z_0$  and  $v_0$ . Execute Step (12).

(11) Assign  $I + 1$  to the number of iterations  $I$ . Assign  $0.5r$  to the step size for search  $r$ , and execute Step (12).

(12) Determine whether the number of columns of the position record matrix  $W_{ac}$  is equal to 0. If true, execute Step (13). If not, execute Step (14).

(13) Assign the element number  $W_z$  to the first element of the position record matrix  $W_{ac}$ , and execute Step (4).

(14) Determine whether the number of columns of the position record matrix  $W_{ac}$  is equal to 1. If true, execute Step (15). If not, execute Step (4).

(15) Assign the element number  $W_z$  to the second element of the position record matrix  $W_{ac}$ , and execute Step (16).

(16) Determine whether the first element of the position record matrix  $W_{ac}$  is equal to the second element. If true, execute Step (17). If not, execute Step (18).

(17) Assign  $rQ$  (acceleration coefficient) to the search step size  $r$ . Set the position record matrix  $W_{ac}$  to an empty matrix, and execute Step (4).

(18) Set the position record matrix  $W_{ac}$  to an empty matrix, and execute Step (4).

(19) Record the current  $x_0, y_0, z_0, v_0, R_0$  and  $I$ . Assign the six elements as a row to the first six columns in the first row of the result record matrix  $P$ . The output result records the data in the first row of the matrix  $P$ , which are  $X$ -axis coordinate of the source  $x_{apt}$ ,  $Y$ -axis coordinate of the source  $y_{apt}$ ,  $Z$ -axis coordinate of the source  $z_{apt}$ , the average P-wave velocity  $v_{apt}$ , the global minimum value of the objective function  $R_{apt}$  and the number of iterations  $I$ .

The flowchart of the variable step size accelerated search method is shown in Fig.7.

### 3.3 Comparison with Newton's method

Newton's method is also called tangent method as a numerical algorithm. Its optimization idea is taking the negative gradient direction of the current position as search direction. The closer it is to the target value, the smaller the step size is and the slower the progress is. The comparison between this method and the variable step size accelerated search method is shown in Table 2.

According to Table 2, the variable step size accelerated search method is superior to the Newton's method in terms of calculation speed, the degree of influence for the initial values of parameters, and the adaptability of the algorithm.

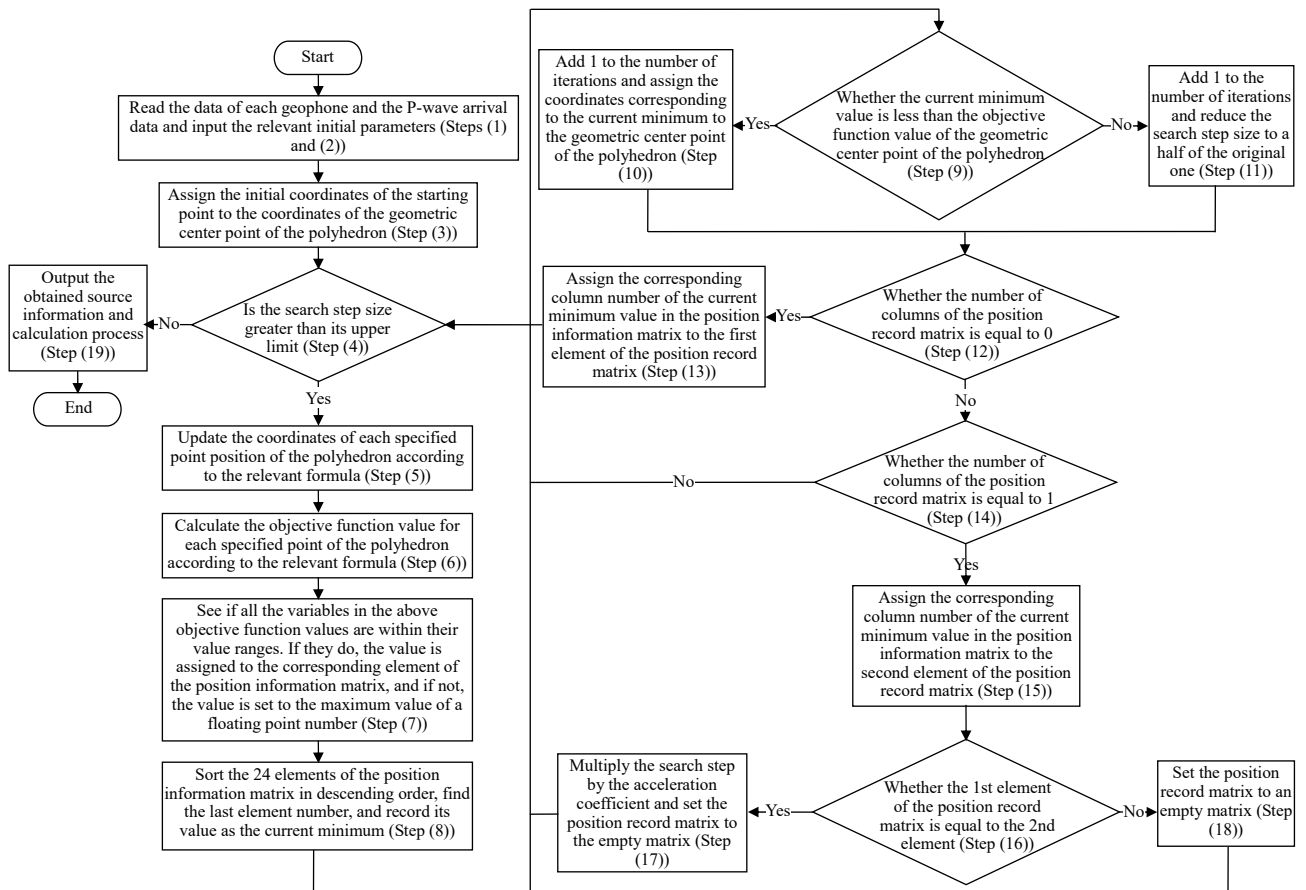


Fig. 7 Flow chart of variable step size accelerated search method

Table 2 Comparison between variable step size accelerated search method and Newton’s method

Comparison items	Locating method		Comparison of results
	Variable step size accelerated search method	Newton’s method	
Convergence stability	The output is the same each time	The output is the same each time	Same effect for both
Accuracy of results	①Output accuracy can be adjusted according to the required accuracy ②The search step size can be gradually reduced according to the search process to ensure the convergence accuracy of the locating results	①Output accuracy can be adjusted according to the required accuracy ②The search step size can be gradually reduced according to the search process to ensure the convergence accuracy of the locating results	Same effect for both
Calculation speed	①Only square root extraction and squaring calculations and addition and subtraction operations are required ②The search step can be changed to achieve accelerated search	①There are a large number of inverse matrix operations of Hessian matrices ②The closer to the end of the search, the smaller the step length and the slower the advance	The former is better than the latter
Degree of influence for initial values of parameters	The initial values of the parameters have no effect on the accuracy of the results and the speed of the calculation	The initial values of the parameters have no effect on the accuracy of the results, but have a significant impact on the calculation speed	The former is better than the latter
Algorithm adaptability	It is only necessary to ensure that the objective function is continuous and the minimum value is unique	As the second order derivative is calculated, it is necessary to ensure the continuity of the first order derivative of the objective function	The former is better than the latter

#### 4 Analysis of simulation examples

In order to demonstrate the effectiveness of the variable step size accelerated search method, we first select two common algorithms for source locating: simulated annealing algorithm and genetic algorithm. Then we analyze and compare the three algorithms through building a simulation

example to simulate the origin of an earthquake, picking the first arrival time and inverting to find the source.

##### 4.1 Building of simulation examples

The model of the example is shown in Fig.8, in which the gray spheres represent the geophones and the small gray cubes represent the sources. A total of eight geophones A, B, C, D, E, F, G, H are set up to form a cube array, a

total of three sources are located inside the arrays I, J, K and a total of three sources are located outside the arrays L, M, N. The coordinates of each point are shown in Tables 3 and 4.

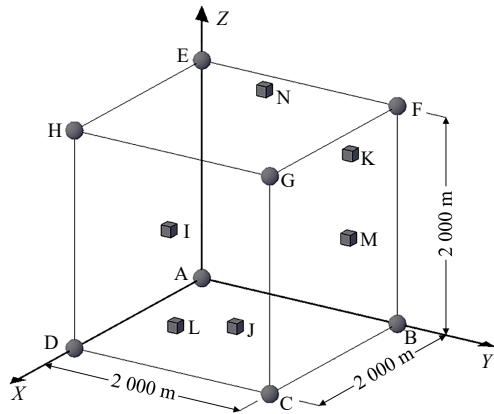


Fig. 8 Schematic diagram of simulation example model

Table 3 Coordinates of geophones in simulation example

Serial number of geophone	Coordinates /m		
	X	Y	Z
A	0	0	0
B	0	2 000	0
C	2 000	2 000	0
D	2 000	0	0
E	0	0	2 000
F	0	2 000	2 000
G	2 000	2 000	2 000
H	2 000	0	2 000

Table 4 Coordinates of each source in simulation example

Serial number of sources	Coordinates /m		
	X	Y	Z
I	1 560	680	1 090
J	1 790	1 510	450
K	150	1 620	1 530
L	2 360	1 270	590
M	1 410	2 420	1 330
N	750	1 130	2 210

Taking the average P-wave velocity of 2 000 m/s and the origin time of 0 s as a reference, we calculate the first arrival time of P-wave according to the distance from each source to the geophone. The results are shown in Table 5.

4.2 Characteristic analysis of proposed search method

The convergence stability, accuracy of result, calculation speed and the degree of influence for the initial values of parameters are the important indicators to determine whether the algorithm can be put into practice. Therefore, based on this standard, we evaluate the advantages and disadvantages of the three algorithms using sets of locating results in single- and multi-source conditions.

Table 5 First arrival time of P-wave in a simulated example

Serial number of geophone	First arrival time of P-wave /s					
	Source I	Source J	Source K	Source L	Source M	Source N
A	1.010 458	1.192 340	1.116 669	1.372 097	1.550 274	1.296 486
B	1.158 026	0.954 817	0.791 802	1.269 902	0.991 640	1.245 341
C	0.883 756	0.348 819	1.215 298	0.502 643	0.757 199	1.341 967
D	0.678 988	0.794 780	1.448 085	0.722 945	1.411 860	1.389 559
E	0.964 896	1.404 163	0.846 729	1.514 150	1.439 913	0.686 203
F	1.118 492	1.208 998	0.311 368	1.422 199	0.808 301	0.583 845
G	0.831 279	0.819 558	0.973 114	0.814 033	0.493 305	0.768 684
H	0.609 118	1.087 049	1.251 779	0.965 738	1.289 709	0.849 044

4.2.1 Analysis of locating results in single- and multi-source conditions

According to the model size, following values are input: the initial coordinates of the starting point  $X_0 = 1\ 000\ m$ ,  $Y_0 = 1\ 000\ m$ ,  $Z_0 = 1\ 000\ m$ ; the initial value of the average P-wave velocity  $V_0 = 1\ 000\ m/s$ ; the upper limits of the model size  $X_u = 2\ 500\ m$ ,  $Y_u = 2\ 500\ m$ ,  $Z_u = 2\ 500\ m$ ; the lower limits of the model size  $X_d = 0\ m$ ,  $Y_d = 0\ m$ ,  $Z_d = 0\ m$ ; the upper speed limit  $V_u = 2\ 500\ m/s$ ; the lower speed limit  $V_d = 0\ m/s$ ; the lower limit of the search step size  $J = 0.01\ m$ ; and the initial value of the search step size  $r = 1\ 000\ m$ . The calculation is carried out by the computer with central processing unit Intel Core I3-4150 CPU @ 3.5 GHz.

(1) Locating results in single-source condition

By inputting the real arrival time data of source K, we use three algorithms to locate the source for 10 times. The locating results are shown in Table 6.

From Table 6, we find that the closer the objective function value is to 0, the closer the calculation result is to the true value of the source (150 m, 1 620 m, 1 530 m) and the true value of the average P-wave velocity is 2 000 m/s. The effect of the three algorithms is shown in Table 7.

(2) Locating results in multi-source condition

We use three algorithms to locate all the sources. The results are shown in Table 8, in which the numbers are the averages of 10 calculation results.

Comparing the locating results of the three algorithms in Table 8 and the true value of each source in Table 4, we show the comparison of the effects of the three algorithms in Table 9.

4.2.2 Convergence stability

In single-source locating condition, it is easy to observe the convergence stability of each calculation of each algorithm. From Table 7, we find that the standard deviations of the objective function value, the locating error and

**Table 6 Locating results of three algorithms under source K**

Algorithm	No. of times	Calculation result					
		Objective function value	X-axis coordinate of sources /m	Y-axis coordinate of sources /m	Z-axis coordinate of sources /m	Average wave velocity /( $m \cdot s^{-1}$ )	Calculation time /s
Simulated annealing algorithm	1	$3.708 \times 10^{-2}$	604.919 4	1 298.801 4	1 265.936 1	966.719 7	0.524 4
	2	$5.296 \times 10^{-3}$	161.353 8	1 609.903 4	1 504.156 3	1 946.540 9	1.129 1
	3	$3.136 \times 10^{-3}$	170.433 0	1 596.184 2	1 513.469 5	1 939.152 6	1.927 6
	4	$2.891 \times 10^{-2}$	509.714 5	1 371.950 4	1 338.503 3	1 238.339 6	0.639 2
	5	$1.836 \times 10^{-2}$	386.129 0	1 454.042 8	1 392.666 0	1 476.172 3	0.818 6
	6	$1.459 \times 10^{-2}$	335.108 0	1 498.476 6	1 447.878 9	1 637.798 6	0.545 2
	7	$2.303 \times 10^{-2}$	447.218 7	1 424.248 2	1 358.481 0	1 361.657 5	1.233 7
	8	$2.335 \times 10^{-3}$	125.823 4	1 641.976 4	1 540.106 7	2 052.868 3	1.949 3
	9	$3.962 \times 10^{-2}$	639.464 6	1 275.845 6	1 249.063 8	909.229 5	0.422 9
	10	$2.353 \times 10^{-3}$	182.144 1	1 597.738 7	1 511.192 6	1 930.216 9	1.367 3
Genetic algorithm	1	$6.907 \times 10^{-3}$	245.818 2	1 556.720 4	1 478.071 6	1 795.807 5	0.195 7
	2	$1.705 \times 10^{-2}$	319.071 8	1 559.325 1	1 455.356 5	1 707.835 2	0.183 7
	3	$3.362 \times 10^{-3}$	197.682 2	1 587.999 3	1 505.493 3	1 899.535 5	0.189 8
	4	$1.035 \times 10^{-2}$	293.320 8	1 529.332 4	1 458.230 1	1 707.275 8	0.176 0
	5	$3.485 \times 10^{-3}$	198.842 3	1 587.205 8	1 503.799 6	1 895.336 7	0.178 0
	6	$1.303 \times 10^{-2}$	325.918 8	1 503.794 6	1 434.092 1	1 623.506 7	0.193 2
	7	$1.408 \times 10^{-2}$	338.634 5	1 493.725 5	1 424.942 9	1 594.250 0	0.181 7
	8	$1.702 \times 10^{-3}$	174.759 1	1 604.366 9	1 516.862 0	1 948.777 9	0.180 5
	9	$1.874 \times 10^{-2}$	398.078 2	1 459.737 7	1 394.971 3	1 474.472 9	0.197 4
	10	$4.633 \times 10^{-2}$	397.386 1	1 571.519 2	1 476.008 9	1 821.211 8	0.176 7
Variable step size accelerated search method	1	$7.265 \times 10^{-6}$	150.103 9	1 619.927 6	1 529.946 3	1 999.780 6	0.056 7
	2	$7.265 \times 10^{-6}$	150.103 9	1 619.927 6	1 529.946 3	1 999.780 6	0.058 0
	3	$7.265 \times 10^{-6}$	150.103 9	1 619.927 6	1 529.946 3	1 999.780 6	0.056 4
	4	$7.265 \times 10^{-6}$	150.103 9	1 619.927 6	1 529.946 3	1 999.780 6	0.056 3
	5	$7.265 \times 10^{-6}$	150.103 9	1 619.927 6	1 529.946 3	1 999.780 6	0.056 0
	6	$7.265 \times 10^{-6}$	150.103 9	1 619.927 6	1 529.946 3	1 999.780 6	0.055 9
	7	$7.265 \times 10^{-6}$	150.103 9	1 619.927 6	1 529.946 3	1 999.780 6	0.059 5
	8	$7.265 \times 10^{-6}$	150.103 9	1 619.927 6	1 529.946 3	1 999.780 6	0.056 0
	9	$7.265 \times 10^{-6}$	150.103 9	1 619.927 6	1 529.946 3	1 999.780 6	0.055 8
	10	$7.265 \times 10^{-6}$	150.103 9	1 619.927 6	1 529.946 3	1 999.780 6	0.055 8

**Table 7 Locating effects of three algorithms under source K**

Algorithm	Objective function value		Locating error /m		Wave velocity error /( $m \cdot s^{-1}$ )		Calculation time /s	
	Average value	Standard deviation	Average value	Standard deviation	Average value	Standard deviation	Average value	Standard deviation
Simulated annealing	$1.747 \times 10^{-2}$	$1.436 \times 10^{-2}$	284.829 8	247.729 1	464.704 0	408.978 1	1.055 7	0.564 2
Genetic algorithm	$1.350 \times 10^{-2}$	$1.297 \times 10^{-2}$	172.793 6	97.906 7	253.198 9	152.694 4	0.185 2	0.008 1
Variable step size	$7.265 \times 10^{-6}$	0	0.137 5	0	0.219 3	0	0.056 6	0.001 2

Note: Locating error is the absolute distance from the calculated source to the real source.

the wave velocity error of the proposed search method are all 0, which are smaller than those of the other two algorithms. Therefore, the convergence stability of the proposed search method is better than that of the other two algorithms.

4.2.3 Accuracy of results

In multi-source locating condition, it is easy to observe the accuracy of each algorithm on source locating. From Table 9, we find that the average of the objective function value of the proposed search method is 0.3% and 0.4% of that of the simulated annealing algorithm and the genetic algorithm, respectively. The average of locating error of the proposed search method is 0.7% and 1.9% of that

of the simulated annealing algorithm and the genetic algorithm, respectively. The average wave velocity error of the proposed search method is 0.8% and 1.8% of that of the simulated annealing algorithm and the genetic algorithm, respectively. Therefore, the proposed search method outperforms the other two algorithms in the accuracy of the result.

4.2.4 Calculation speed

From Table 9, we find that the average of calculation time of the proposed search method is 6.9% and 33.2% of that of the simulated annealing algorithm and the genetic algorithm, respectively. The standard deviation of the calculation time is 0.2% and 14.8% of that of the simulated

**Table 8 Locating results of three algorithms for all sources**

Algorithm	Serial number of sources	Calculation result					
		Objective function value	X-axis coordinate of sources /m	Y-axis coordinate of sources /m	Z-axis coordinate of sources /m	Average wave velocity /( $m \cdot s^{-1}$ )	Calculation time /s
Simulated annealing algorithm	I	$4.114 \times 10^{-3}$	1 440.191 6	749.157 6	1 072.190 1	1 578.482 9	0.883 2
	J	$1.431 \times 10^{-2}$	1 403.569 3	567.639 2	1 574.812 1	1 403.569 3	1.204 9
	K	$1.538 \times 10^{-2}$	327.082 0	1 500.777 8	1 426.471 0	1 615.267 5	1.004 3
	L	$1.343 \times 10^{-2}$	1 777.316 9	1 163.607 0	754.971 3	1 268.054 7	0.821 8
	M	$1.151 \times 10^{-2}$	1 261.499 2	1 854.309 2	1 210.512 5	1 358.642 2	0.888 6
	N	$7.392 \times 10^{-3}$	850.546 7	1 078.317 1	1 685.402 5	1 253.205 9	0.644 1
Genetic algorithm	I	$1.039 \times 10^{-3}$	1 558.746 5	680.947 2	1 089.825 2	1 994.252 4	0.174 8
	J	$8.159 \times 10^{-3}$	1 744.595 9	1 470.897 1	486.907 3	1 890.970 9	0.212 4
	K	$1.507 \times 10^{-2}$	309.796 1	1 520.563 8	1 458.454 8	1 682.961 9	0.187 3
	L	$9.974 \times 10^{-3}$	2 014.780 2	1 221.830 3	684.709 7	1 620.121 0	0.183 9
	M	$1.283 \times 10^{-2}$	1 319.899 4	2 044.905 3	1 258.441 1	1 654.805 2	0.187 9
	N	$3.561 \times 10^{-3}$	803.677 2	1 103.360 4	1 931.302 6	1 634.386 1	0.183 5
Variable step size accelerated search method	I	$3.416 \times 10^{-5}$	1 558.665 1	680.726 5	1 089.803 9	1 995.552 3	0.057 2
	J	$9.579 \times 10^{-6}$	1 789.859 1	1 509.919 0	450.091 4	1 999.678 6	0.062 7
	K	$7.265 \times 10^{-6}$	150.103 8	1 619.927 6	1 529.946 3	1 999.780 6	0.056 6
	L	$4.493 \times 10^{-5}$	2 354.384 8	1 268.992 8	591.573 3	1 994.840 9	0.080 1
	M	$5.137 \times 10^{-5}$	1 412.250 2	2 428.274 2	1 331.786 2	2 006.882 8	0.071 4
	N	$6.288 \times 10^{-5}$	751.537 9	1 129.211 6	2 201.659 4	1 990.317 6	0.047 6

**Table 9 Comparison of three algorithms for locating all sources**

Algorithm	Objective function value		Locating error /m		Wave velocity error /( $m \cdot s^{-1}$ )		Calculation time /s	
	Average value	Standard deviation	Average value	Standard deviation	Average value	Standard deviation	Average value	Standard deviation
	Simulated annealing algorithm	$1.102 2 \times 10^{-2}$	$4.398 5 \times 10^{-3}$	607.099 6	445.210 2	587.129 5	153.547 1	0.907 8
Genetic algorithm	$8.438 \times 10^{-3}$	$5.371 \times 10^{-3}$	218.653 1	143.936 3	253.750 4	156.996 1	0.188 3	0.012 7
Variable step size accelerated search method	$3.503 \times 10^{-5}$	$2.263 \times 10^{-5}$	4.175 1	3.699 1	4.452 1	3.707 9	0.062 6	0.010 5

annealing algorithm and the genetic algorithm, respectively. Therefore, the proposed search method outperforms the other two algorithms in both the calculation speed and the stability of calculation time.

4.2.5 Degree of influence for initial values of parameters

In the case of merely changing one initial value of parameter at a time and ensuring other parameters equal to their initial values, the initial coordinates of the starting points are  $X_0 = 1\ 000\ m$ ,  $Y_0 = 1\ 000\ m$ ,  $Z_0 = 1\ 000\ m$ , the initial value of the average P-wave velocity is  $V_0 = 1\ 000\ m/s$ , the lower limit of the search step size is  $J = 0.001\ m$  and the initial value of the search step size is  $r = 1\ 000\ m$ . Taking the source K as an example, we analyze the locating error when the parameters have different initial values. The initial value ranges from 100 m to 2 900 m. Under the condition that the target parameters change independently, the locating errors corresponding to different initial values of other parameters are shown in Fig.9, in which the numbers are the averages of 10 calculation results.

As the range of the lower limit of the search step size

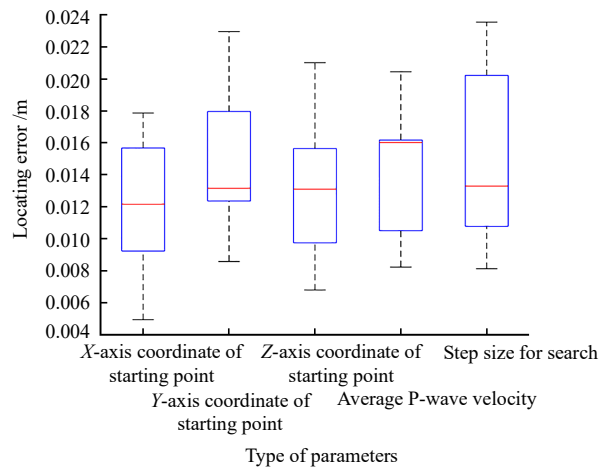


**Fig. 9 Locating errors of each parameter with different initial values**

$J$  is different from that of the above parameters, it is analyzed separately below. Under the condition that other parameters are unchanged and the search step size  $J$  varies from  $1 \times 10^{-12}\ m$  to 100 m, the calculation results are tabulated in Table 10.

Based on Fig.9 and Table 10, we draw the following conclusions:

**Table 10 Locating results under different initial values of lower limit of search step size**

Initial value	Calculation result					
	Objective function value	X-axis coordinate error /m	Y-axis coordinate error /m	Z-axis coordinate error /m	Wave velocity error /( $m \cdot s^{-1}$ )	Calculation time /s
$1 \times 10^{-12}$	$1.416 \times 10^{-10}$	$3.620 \times 10^{-7}$	$4.939 \times 10^{-7}$	$8.889 \times 10^{-8}$	$1.404 \times 10^{-6}$	0.165 1
$1 \times 10^{-11}$	$1.416 \times 10^{-10}$	$3.620 \times 10^{-7}$	$4.939 \times 10^{-7}$	$8.889 \times 10^{-8}$	$1.404 \times 10^{-6}$	0.165 6
$1 \times 10^{-10}$	$1.416 \times 10^{-10}$	$3.620 \times 10^{-7}$	$4.939 \times 10^{-7}$	$8.889 \times 10^{-8}$	$1.404 \times 10^{-6}$	0.164 9
$1 \times 10^{-9}$	$1.416 \times 10^{-10}$	$3.643 \times 10^{-7}$	$4.930 \times 10^{-7}$	$8.960 \times 10^{-8}$	$1.409 \times 10^{-6}$	0.157 3
$1 \times 10^{-8}$	$1.416 \times 10^{-10}$	$2.972 \times 10^{-7}$	$5.340 \times 10^{-7}$	$5.409 \times 10^{-8}$	$1.270 \times 10^{-6}$	0.148 4
$1 \times 10^{-7}$	$1.711 \times 10^{-10}$	$1.071 \times 10^{-6}$	$1.426 \times 10^{-6}$	$6.435 \times 10^{-7}$	$1.493 \times 10^{-6}$	0.147 4
$1 \times 10^{-6}$	$9.968 \times 10^{-10}$	$1.424 \times 10^{-5}$	$1.017 \times 10^{-5}$	$7.266 \times 10^{-6}$	$2.823 \times 10^{-5}$	0.134 9
$1 \times 10^{-5}$	$8.699 \times 10^{-9}$	$1.248 \times 10^{-4}$	$8.634 \times 10^{-5}$	$6.428 \times 10^{-5}$	$2.623 \times 10^{-4}$	0.115 0
$1 \times 10^{-4}$	$1.206 \times 10^{-7}$	$1.724 \times 10^{-3}$	$1.198 \times 10^{-3}$	$9.108 \times 10^{-4}$	$3.651 \times 10^{-3}$	0.091 6
$1 \times 10^{-3}$	$3.742 \times 10^{-7}$	$5.282 \times 10^{-3}$	$3.582 \times 10^{-3}$	$2.377 \times 10^{-3}$	$1.092 \times 10^{-2}$	0.086 3
$1 \times 10^{-2}$	$7.265 \times 10^{-6}$	$1.038 \times 10^{-1}$	$0.723 \times 10^{-1}$	$0.536 \times 10^{-1}$	$2.193 \times 10^{-1}$	0.056 6
$1 \times 10^{-1}$	$5.622 \times 10^{-5}$	$8.026 \times 10^{-1}$	$5.595 \times 10^{-1}$	$4.045 \times 10^{-1}$	$16.902 \times 10^{-1}$	0.045 6
$1 \times 10^0$	$9.907 \times 10^{-4}$	$145.113 \times 10^{-1}$	$90.617 \times 10^{-1}$	$76.378 \times 10^{-1}$	$298.722 \times 10^{-1}$	0.024 6
$1 \times 10^1$	$9.907 \times 10^{-4}$	$265.250 \times 10^{-1}$	15.100	26.800	65.750	0.024 5
$1 \times 10^2$	$3.793 \times 10^{-3}$	20.000	250.000	340.000	130.000	0.003 6

(1) When the lower limit of the search step size  $J$  is equal to 0.001 m, the influences of changing the initial values of the coordinates of the starting point, the initial value of the average P-wave velocity and the search step size on the locating error are between 0.005 m and 0.025 m.

(2) Reducing the lower limit  $J$  of the search step size can effectively improve the accuracy of the results and increase the calculation time.

(3) The variable step size accelerated search method can calculate the objective function value to  $1.416 \times 10^{-10}$  and minimize the locating error to  $6.188 \times 10^{-7}$  m.

### 5 Verification with project case

In order to further demonstrate the advantages of the variable step size accelerated search method for source locating, we compare the three algorithms in actual case. Using the average wave velocity to simplify the velocity model, we analyze the influences of the first arrival time of P-wave and coordinates of geophone obtained from project case on source locating.

#### 5.1 Coordinates of geophone and first arrival time

Using the data obtained from locating test for the artificial blasting in Shizhuyuan polymetallic mine<sup>[22]</sup>, we compare and analyze the locating effects of the three algorithms. There are 30 geophones arranged on site. After the detonation, eight geophones have received the first arrival time of P-wave. The coordinates of the blasting source measured on site, i.e. the true value of the source, are (8 732.7 m, 6 570.6 m, 511.3 m). The spatial coordinates and the first arrival time of P-wave are shown in Table 11.

**Table 11 Geophone coordinates and first arrival time of P-wave**

Serial number of geophone	Coordinates /m			First arrival time of P-wave /ms
	X	Y	Z	
9	8 761	6 614	522	34.9
21	8 737	6 609	565	36.6
5	8 666	6 600	520	39.3
17	8 668	6 599	565	41.1
4	8 641	6 515	520	42.3
8	8 691	6 684	520	44.5
2	8 721	6 449	520	47.8
26	8 702	6 604	647	50.0

#### 5.2 Case analysis of proposed search method

The  $x_0$ ,  $y_0$  and  $z_0$  are the spatial variables and  $v_0$  is the velocity variable. The images are drawn with two combinations of both spatial variables, and spatial variables and velocity variables. In Figs.10 and 11,  $x_0$  ranges from 0 to 15 000 m,  $y_0$  ranges from 0 to 15 000 m, and  $v_0$  ranges from 3 m/ms to 20 m/ms.

##### 5.2.1 2D image

The number of divisions  $F_s$  in Figs.10 and 11 is 500 and the observation angles are as follows: azimuth of  $-40^\circ$  and pitch angle of  $20^\circ$ .

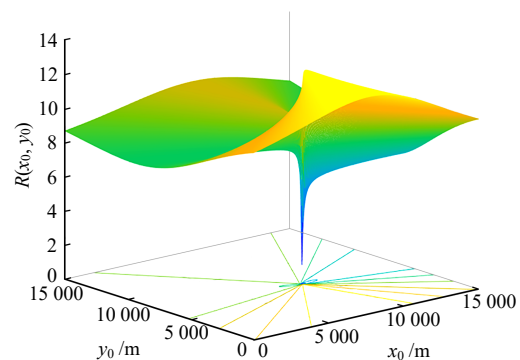


**Fig. 10 Image of  $R(x_0, y_0)$  when  $v_0$  and  $z_0$  are fixed values in engineering case**

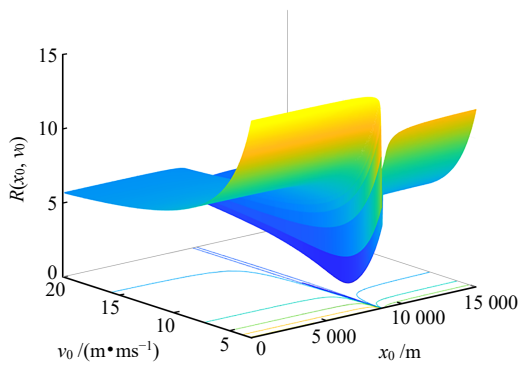


**Fig. 11** Image of  $R(x_0, v_0)$  when  $y_0$  and  $z_0$  are fixed values in engineering case

#### (1) Image of $R(x_0, y_0)$

In Fig.10, we find that when the average P-wave velocity  $v_0 = 6.4772$  m/ms, and the coordinate of source  $Z z_0 = 506.8261$  m, the objective function  $R(x_0, y_0)$  is continuous with a distinct unique minimum value. The objective function value ranges from 0 to 4, the convergence range of  $x_0$  ranges from 8 682 m to 8 845 m, and the convergence range of  $y_0$  is from 6 533 m to 6 624 m.

#### (2) Image of $R(x_0, v_0)$

From Fig.11, we find that when  $y_0 = 6 576.4979$  m and  $z_0 = 506.8261$  m, the image of the objective function  $R(x_0, v_0)$  is still continuous, and there is a unique minimum value. The objective function value ranges from 0 to 2, the convergence range of  $x_0$  is from 8 725 m to 8 765 m, and the convergence range of  $v_0$  is from 4.7 m/ms to 10.2 m/ms.

#### 5.2.2 Comparison between images

By comparing Figs.1 and 10, we find that in Fig.1, when the coordinates of the geophone and the first arrival time of P-wave have no deviation, and the wave velocity is constant, the image of the objective function is in uniform inverted cone shape. The spatial distribution conforms to the features that the objective function is continuous, the minimum value is unique, the uniaxial convergence range is gradually decreasing, and the convergence ranges of each axis are different. Compared to the ideal and standard image in Fig.1, the image in Fig.10 has large distortion, such as the sudden drop of minimum value and some protrusions. But we can still find that starting from any point in the figure, a descending path can be found until it reaches the minimum value of the objective function. Additionally, the closer it is to the minimum value, the smaller the convergence range is. Therefore, the two findings that the objective function is continuous with a unique minimum value, and the uniaxial convergence range is gradually decreasing still hold true.

Comparing Figs.10 and 11, we find that the difference between the two figures is that the independent variables in the former are  $x_0$  and  $y_0$ , while those in the latter are  $x_0$  and  $v_0$ . Comparing the coordinate axes of  $y_0$  and  $v_0$ , we find that the convergence ranges of the two figures are different. Therefore, the finding that the convergence range of each axis is different still holds true.

To sum up, in the complex engineering practice, when the coordinates of the geophone and the first arrival time of P-wave have deviations and the P-wave velocity has serious anisotropy, the above three findings are still applicable.

#### 5.2.3 Analysis of calculation results

Following values are input in this section: the initial coordinates of the starting point  $X_0 = 5 000$  m,  $Y_0 = 5 000$  m,  $Z_0 = 300$  m; the initial value of the average P-wave velocity  $V_0 = 5$  m/ms; the upper limit of the model size  $X_u = 10 000$  m,  $Y_u = 10 000$  m,  $Z_u = 1 000$  m; the lower limit of model size  $X_d = 0$  m,  $Y_d = 0$  m,  $Z_d = 0$  m; the upper speed limit  $V_u = 20$  m/s; the lower speed limit  $V_d = 0$  m/s; the lower limit of search step size  $J = 0.001$  m; and the initial value of the search step size  $r = 3 000$  m. The results of 10 calculations using the variable step size accelerated search method are shown in Table 12.

From Table 13, we find that the averages and standard deviations of the objective function value and the locating error of the proposed search method are smaller than those of the other two algorithms. It indicates that this algorithm outperforms the other two algorithms in the accuracy of result and convergence stability. Additionally, the average calculation time is shorter than that of the other two algorithms, indicating that this algorithm outperforms the other two algorithms in calculation speed.

The minimum points in the images of the objective functions  $R(x_0, y_0)$ ,  $R(x_0, z_0)$  and  $R(x_0, v_0)$  are searched respectively. The objective function values of the minimum points are all 0.9149. The coordinates of the corresponding sources are (8 731.3624 m, 6 576.4978 m, 506.8261 m). It indicates that when the first arrival time of P-wave, the objective function model and the coordinates of geophone are specified, the proposed search method can find the best convergence point quickly and accurately and guarantee that the results are the same every time.

Meanwhile, through the image analysis and the calculation results of the proposed search method, we find that the optimal convergence point of the objective function is unique when the first arrival time of P-wave, the objective function model and the coordinates of geophone are specified. Therefore, the search algorithm has no substantial influence on the locating accuracy. It is mainly influenced

**Table 12 Locating results of the three algorithms**

Algorithm	No. of times	Objective function value	X-axis coordinate of sources /m	Y-axis coordinate of sources /m	Z-axis coordinate of sources /m	Average wave velocity /( $m \cdot ms^{-1}$ )	Calculation time /s
Simulated annealing algorithm	1	6.053 5	4 962.998 6	5 121.246 0	332.171 1	19.998 1	0.314 2
	2	6.092 4	4 984.546 5	5 030.372 9	304.369 4	19.770 4	0.314 0
	3	5.925 4	4 762.522 5	5 451.789 4	178.328 3	19.995 1	0.663 4
	4	5.917 3	4 429.177 4	5 316.901 2	5.455 5	19.969 8	0.533 1
	5	5.879 2	4 721.391 3	5 546.006 8	64.286 2	19.987 7	0.568 4
	6	5.949 0	5 806.302 9	5 512.133 2	31.484 5	19.999 6	0.795 4
	7	6.031 6	4 873.563 0	4 994.925 1	33.491 0	19.999 6	0.369 4
	8	5.824 2	4 612.700 9	5 711.829 0	31.929 7	19.999 2	0.703 1
	9	6.053 0	4 942.672 1	5 050.075 5	217.855 9	19.992 7	0.319 8
	10	5.780 8	4 755.897 0	6 080.043 2	337.084 3	19.993 6	1.262 4
Genetic algorithm	1	4.075 5	9 190.530 2	7 156.015 6	218.762 2	19.966 9	0.173 9
	2	3.094 4	8 828.684 9	6 663.026 9	351.806 9	11.575 0	0.173 1
	3	3.779 7	8 659.098 3	6 641.088 1	365.406 8	12.568 7	0.170 7
	4	5.042 5	6 774.875 4	9 150.004 0	163.928 6	20.000 0	0.179 5
	5	5.085 7	6 704.406 2	9 088.321 7	274.634 8	19.997 9	0.170 1
	6	4.207 1	8 600.788 3	7 020.358 7	119.543 7	19.990 1	0.174 3
	7	5.066 7	7 197.155 0	7 774.567 3	221.522 3	19.998 1	0.184 6
	8	3.405 1	8 978.397 3	6 655.705 6	362.153 3	11.629 6	0.172 7
	9	4.270 0	9 901.636 3	7 122.175 0	366.571 0	19.131 4	0.174 8
	10	3.539 9	9 152.562 1	6 754.492 0	120.568 7	11.972 4	0.174 4
Variable step size accelerated search method	1	0.914 9	8 731.362 4	6 576.497 8	506.826 1	6.477 2	0.111 1
	2	0.914 9	8 731.362 4	6 576.497 8	506.826 1	6.477 2	0.119 1
	3	0.914 9	8 731.362 4	6 576.497 8	506.826 1	6.477 2	0.117 6
	4	0.914 9	8 731.362 4	6 576.497 8	506.826 1	6.477 2	0.118 9
	5	0.914 9	8 731.362 4	6 576.497 8	506.826 1	6.477 2	0.116 5
	6	0.914 9	8 731.362 4	6 576.497 8	506.826 1	6.477 2	0.133 2
	7	0.914 9	8 731.362 4	6 576.497 8	506.826 1	6.477 2	0.135 0
	8	0.914 9	8 731.362 4	6 576.497 8	506.826 1	6.477 2	0.110 4
	9	0.914 9	8 731.362 4	6 576.497 8	506.826 1	6.477 2	0.126 9
	10	0.914 9	8 731.362 4	6 576.497 8	506.826 1	6.477 2	0.116 6

**Table 13 Comparison of locating effect of three algorithms**

Algorithm	Objective function value		Locating error /m		Calculation time /s	
	Average value	Standard deviation	Average value	Standard deviation	Average value	Standard deviation
Simulated annealing algorithm	5.950 6	0.105 1	4 059.861 0	350.224 1	0.584 3	0.296 2
Genetic algorithm	4.156 7	0.723 7	1 246.928 0	1 187.398 2	0.174 8	0.004 2
Variable step size accelerated search method	0.914 9	0	7.522 6	0	0.120 5	0.008 4

by other factors, such as the first arrival time of P-wave, the objective function model, the coordinates of geophone and the wave velocity model.

### 6 Conclusions

We use the variable step size accelerated search method, simulated annealing algorithm and genetic algorithm to locate the microseismic source in the simulation example. We compare and analyze the advantages of the variable step size accelerated search method, which is also verified by project case. The main conclusions are drawn as follows:

(1) The objective function of microseismic locating is continuous within the monitoring range and has a unique minimum value. The uniaxial convergence range is gradually decreasing and the convergence range of each axis is

different. Therefore, the search algorithm only needs to iteratively compare the objective function values starting from a certain point until it reaches the minimum of the objective function; the closer the iteration factor is to the source, the smaller the required search step size, thus the search step size should adapt to the change of the convergence range. The convergence range of each unknown of the objective function is different, thus the search algorithm should adopt different search step sizes for the search of each axis and should adapt to the convergence range of each unknown.

(2) In the simulation example, comparing with the simulated annealing algorithm and the genetic algorithm, the standard deviations of the objective function value, the locating error and the wave velocity error of the proposed search method are all 0. The average of the locating

error of the proposed search method is 0.7% and 1.9% of that of the other two algorithms, respectively. The average calculation time of the proposed search method is 6.9% and 33.2% of that of the other two algorithms, respectively.

(3) When the initial values of the parameters in the proposed search method are specified, the effect of merely changing one parameter on locating error is from 0.005 m to 0.025 m. Reducing the lower limit of the search step size can effectively improve the accuracy of the results and increase the corresponding calculation time.

(4) The optimum convergence point of the objective function is unique when the first arrival time of P-wave, the objective function model and the coordinates of geophone are specified. Therefore, the search algorithm has no substantial influence on the locating accuracy.

In the case of limited observation conditions and only the simplified velocity model can be used in engineering project, the search method proposed in this paper outperforms the conventional methods in source locating. For the application of the non-uniform velocity model, it needs further research with test data.

## References

- [1] PAN Yi-shan, ZHAO Yang-feng, GUAN Fu-hai, et al. Study on rockburst monitoring and orientation system and its application[J]. Chinese Journal of Rock Mechanics and Engineering, 2007, 26(5): 1002–1011.
- [2] CUI Feng, YANG Yan-bin, LAI Xing-ping, et al. Similar material simulation experimental study on rockbursts induced by key stratum breaking based on microseismic monitoring[J]. Chinese Journal of Rock Mechanics and Engineering, 2019, 38(4): 803–814.
- [3] LI Jin-yu, LEI Wen-jie, ZHAO Hong-bao, et al. Microseismic characteristics during impact failure of coal and rock under repetitive blast mining[J]. Journal of China University of Mining & Technology, 2019, 48(5): 966–974.
- [4] LI Xiang, XU Nu-wen. Research developments and prospects on microseismic source location[J]. Progress in Geophysics, 2020, 35(2): 598–607.
- [5] CHEN Bing-ru, FENG Xia-ting, FU Qi-qing, et al. Integration and high precision intelligence microseismic monitoring technology and its application in deep rock engineering[J]. Rock and Soil Mechanics, 2020, 41(7): 2422–2431.
- [6] JIANG Ruo-chen, XU Nu-wen, DAI Feng, et al. Research on microseismic location based on fast marching upwind linear interpolation method[J]. Rock and Soil Mechanics, 2019, 40(9): 3697–3708.
- [7] LI Nan, WANG En-yuan, SUN Zhen-yu, et al. Simplex microseismic source location method based on L1 norm statistical standard[J]. Journal of China Coal Society, 2014, 39(12): 2431–2438.
- [8] JIA Bao-xin, JIA Zhi-bo, ZHAO Pei, et al. Microseismic location in local scale region based on high-density array[J]. Chinese Journal of Geotechnical Engineering, 2017, 39(4): 705–712.
- [9] WANG Yun-hong, WANG Bao-li, DUAN Jian-hua. Microseismic positioning method based on differential evolution algorithm[J]. Coal Geology & Exploration, 2019, 47(1): 168–173, 180.
- [10] WANG Hui, LIANG Miao, ZHU Meng-bo. A hybrid microseismic source location algorithm based on simplex and shortest path ray tracing[J]. China Mining Magazine, 2020, 29(10): 110–115, 121.
- [11] JIANG Tian-qi, PEI Shuo-jin. Micro-seismic event location based on Newton iteration method and grid-search method[J]. Journal of Mining Science and Technology, 2019, 4(6): 480–488.
- [12] SOLEDAD R L, DANILO R V. Microseismic event location using global optimization algorithms an integrated and automated workflow[J]. Journal of Applied Geophysics, 2018, 149(1): 18–24.
- [13] NEALE J W, HARMON N, SROKOSZ M. Improving microseismic P-wave source location with multiple seismic arrays[J]. Journal of Geophysical Research: Solid Earth, 2018, 123(1): 476–492.
- [14] XIAO T, WEI Z, JIE Z. Cross double-difference inversion for simultaneous velocity model update and microseismic event location[J]. Geophysical Prospecting, 2017, 65(Suppl.1): 259–273.
- [15] NAN L, MAOCHEN G, ENYUAN W, et al. The influence mechanism and optimization of the sensor network on the MSAE source location[J]. Shock and Vibration, 2020(Suppl.1): 1–16.
- [16] TIAN Yue, CHEN Xiao-fei. Review of seismic location study[J]. Progress in Geophysics, 2002, 17(1): 147–155.
- [17] WANG Zhi-gang. The mechanism and effect analysis of using dual waves in source location[D]. Beijing: China University of Mining & Technology, Beijing, 2018.
- [18] JIA Bao-xin, ZHAO Pei, JIANG Ming, et al. Three-dimensional propagation model building in heterogeneous medium of mine earthquake shock wave and its application[J]. Journal of China Coal Society, 2014, 39(2): 364–370.
- [19] LI Luo-lan, HE Chuan, TAN Yu-yang. Study of recording system and objective function for microseismic source location[J]. Acta Scientiarum Naturalium Universitatis Pekinensis, 2017, 53(2): 329–343.
- [20] DONG Long-jun, LI Xi-bing, MA Ju, et al. Three-dimensional analytical comprehensive solutions for acoustic emission/microseismic sources of unknown velocity system[J]. Chinese Journal of Rock Mechanics and Engineering, 2017, 36(1): 186–197.
- [21] ZHANG Yuan-sheng, GAO Yong-tao, WANG Zhe, et al. Microseismic positioning based on an SA-PSO hybrid algorithm[J]. Modern Tunnelling Technology, 2016, 53(3): 137–145.
- [22] LIN Feng, LI Shu-lin, XUE Yun-liang, et al. Microseismic sources location methods based on different initial values[J]. Chinese Journal of Rock Mechanics and Engineering, 2010, 29(5): 996–1002.